Journal of Electrostatics 132 (2024) 103986

Contents lists available at ScienceDirect

Journal of Electrostatics

journal homepage: www.elsevier.com/locate/elstat

Electrostatic potential measurement of floating conductive objects: Some theoretical considerations and experimental results

Pedro Llovera-Segovia [a,b,*], Philippe Molinié [c], Vicente Fuster-Roig [a,b], Alfredo Quijano-López [a,b]

[a] Instituto de Tecnología Eléctrica - Universitat Politècnica de València Spain
[b] Instituto Tecnológico de la Energía (ITE), Spain
[c] Laboratoire de Génie Electrique et Electronique de Paris (GeePs), Université Paris-Saclay, CentraleSupélec, CNRS France

ARTICLE INFO

Keywords:
Electrostatic potential
Field mill
feedback probe
Floating object
Voltage decay

ABSTRACT

The measurement of electrostatic potentials of floating conductive objects can, in principle, be performed by well-known basic experimental setups. Commercial equipment is readily available and the physical principles underlaying the problem are well established. However, electrostatic measurements require special attention, as significant errors can arise from the influence of the measuring setup or the misinterpretation of the results. First, the specificity of the measuring equipment must be well understood such as the difference between field mills, induction probes and feedback probes (also called electrostatic probes). These instruments create specific boundary conditions around the object being measured such as the introduction of grounded planes or the cancellation of the electric field. This influence is particularly significant when measuring floating objects as, for example, belts and suspended or flying objects. Even when results are provided directly in volts, their interpretation varies greatly depending on the instrument used. In the case of the field mills measurements, a calibration must be performed to convert the measured electric field into the potential of the floating object. This calibration is often performed by applying a known potential to the floating object. However, this procedure may introduce errors in the measured values due to the presence of the high voltage cable used to charge the object. We describe some examples of numerical calculations and show some experimental measurements on a levitating object.

1. Introduction

Measuring the electrostatic potential of floating objects, or objects completely insulated from ground is of interest in many applications such as aircrafts or atmospheric electric measurements. Charge accumulation in aircrafts leads to corona discharges and communication interferences or increased risk during in-flight refueling operation. In recent years, the electrostatic charge of aircrafts or unmanned aerial vehicles has been investigated using on-board field mills [1]. The charging of a moving floating object is primarily due to friction with particles in the air (clean air does not lead to electrostatic charging), while discharging can occur through interaction with ions in the air, corona discharge or electric discharges appearing on the object or its surroundings.

An experimental reproduction of these phenomena on floating objects can be achieved by supporting them with insulators or insulating strings, although this approach inevitably introduces several kinds of perturbations due to the relative permittivity or conductivity of the insulating materials, which may dissipate or screen part of the static charge. These effects may be negligible on the time scale of short experiments, but their influence should be carefully assessed for proper analysis in long-term measurements. An alternative is to use setups that involve actual levitating objects.

In general, the potential decay of an object or surface is measured to assess the dissipation property of a material or to determine the time constant of a process for safety reasons. From a physical perspective, the electrostatic charge dissipation of a charged body can involve simultaneous processes [2,3]. The interpretation of electrostatic charge dissipation mechanisms must be conducted with care, considering the predominant physical processes involved.

This paper focuses on electrostatic field and potential measurements on floating objects such as levitating objects, as well as on aircrafts or

* Corresponding author. Instituto de Tecnología Eléctrica - Universitat Politècnica de València Spain.
E-mail address: pllovera@ite.upv.es (P. Llovera-Segovia).

https://doi.org/10.1016/j.elstat.2024.103986
Received 29 December 2023; Received in revised form 26 September 2024; Accepted 29 September 2024
Available online 18 October 2024

objects isolated from ground. Electrostatic field and electrostatic potential measurements are fundamental to the analysis of any electrostatic problem, but they must be performed with caution to avoid misunderstandings or significant errors. Non-contact instruments such as field mills or feedback probes are widely used to measure the electrostatic potential of objects. If a measurement is solely focused on the time constants of the discharge process, relative values of the measured variables (electrostatic field or potential) may suffice. However, when investigating the exact value of the electrostatic potential of a floating object certain precautions must be taken. In this paper, we analyze the influence of the measuring instrument on the measured value, as well as the specific challenges of voltage calibration of floating conductive objects when using field mills.

2. Electrostatic instruments

The application of Gauss's law to the surface of a conductive body exposed to an existing electric field leads to a well-known relationship between the electric field in the air and the surface charge density induced on the surface:

$$\sigma = \varepsilon_0 E \tag{1}$$

where σ is the charge density on the surface, ε_0 is the dielectric permittivity of air and E is the electric field in the air. If this surface charge can be measured, it becomes straightforward to obtain the value of the electric field at that point. To achieve this, a small conductive surface (the sensing area) can be placed in a location where the disturbance to the electric field is negligible. The total induced charge Q on the surface S is measured:

$$Q = \sigma S \tag{2}$$

For small sensing areas, the electric field at their surface can be approximated to:

$$E \approx \frac{Q}{S\varepsilon_0} \tag{3}$$

Measurement of the total induced charge Q on the sensing area can be carried out using current integration in a capacitor, an electronic integration circuit or by numerical integration. However, long-term electrostatic charge measurements using integration techniques are challenging due to leakage currents in insulating materials [3] or in electronic components and circuits (see, for example, application notes of ultra-low bias current operational amplifiers such as OP 128 for electrometers). Leakage or bias currents in the range of 75 fA can lead to a drift in long-term current integration, which cannot be avoided. Instruments based on direct measurement of induced charge are thus typically designed for short-term measurements and need to be reset under zero-field conditions before each measurement. These short-term measurement field meters are generally handheld, and their metallic casings are typically grounded.

The field mill offers a solution to the drift problem in static electric field measurements ([4] chapter 11), by periodically providing a zero-field condition that can be used as a reference. The sensing area is placed inside a conductive enclosure with a window that is alternatively open or closed by a grounded moving conductive metal piece. This system automatically performs the zero-reference procedure that was manually required for short-term measurement field meters. Calibration of the instrument under controlled conditions is also necessary [5].

The measurement drift problem can also be resolved using a Kelvin-Zisman probe ([4] chapter 11). This device continuously adapts the probe voltage to the surface potential of the measured object through an active feedback loop by ensuring the cancellation of the electric field seen by the sensing electrode. The sensing area oscillates at high frequency in a direction perpendicular to its surface, driven by a piezoelectric actuator. Although the probe is exposed to a static electric field, the movement of the sensing area induces a variable charge on its surface, which generates an alternating current that can be measured. A feedback circuit controlling a high voltage amplifier is designed to cancel the AC current produced by the oscillation, by adjusting the potential of the surrounding metallic enclosure of the sensing electrode. When the probe is brought near a surface, the voltage of the probe is modified until the electric potential difference across the gap between the charged surface and the metallic probe is zero. Feedback probes are usually small and need to be positioned close to the surface being measured.

There are significant differences between using field mills and feedback probes in electrostatic measurements [6] and special care must be taken when dealing with floating objects [7]. Although this issue is relatively known, some misinterpretations persist. We will show the influence of the instruments on the measured values through theoretical and numerical modelling applied to an example of floating conductive spheres. We will also suggest some precautions that should be taken in section 3.

Electrostatic probes provide a direct measurement of surface potential. However, when the potential is too high, the charged object is far from the ground, or when the potential of a flying object needs to be measured from the object itself (as in the case of an aircraft) using a field mill is often the only viable solution.

In such cases, evaluating the potential from the field measurement requires calculations, which can be complex. An experimental calibration is typically required. The object is charged to a known potential, and the electric field under these conditions is measured. From this calibration point, assuming no other changes in the experimental configuration except for the electrostatic charge on the floating object, the electrostatic potential can be determined by linearity. However, this assumption introduces a logical contradiction, as it is impossible to perform a calibration on a flying object without altering the experimental setup. In section 4, we analyze practical errors introduced by the calibration procedure when estimating the potential.

3. Influence of the measuring instrument

3.1. Influence of a field meter

Let's simplify the experimental setup to two conductive bodies over a grounded surface: one floating, carrying a charge Q (the object under study), and the other grounded (either a field mill or a short-term measurement field meter). Let's also consider the case where the measurement instrument is removed, without altering the charge on the conductive body. Both scenarios are shown in Fig. 1. We may write:

$$V_0 = \frac{Q}{C_{10}} \text{ and } V_1 = \frac{Q}{C_{11} + C_{12}} \tag{4}$$

Where V_0 is the potential of the conductive body alone, and C_{10} its capacitance to the ground, V_1 is the potential of the conductive body influenced by the field sensor, C_{11} its capacitance to the ground and C_{12} the capacitance between the sphere and the instrument.

Since the field meter intercepts some of the electric field lines emitted by the charged body and also reduces their length, we have:

$$C_{11} < C_{10} < C_{11} + C_{12} \text{ and } V_1 < V_0 \tag{5}$$

As a result, the electrostatic potential of the charged object may be significantly altered by the presence of the field meter, depending on the distance to the ground and the relative size of the object compared to the instrument.

To illustrate this effect, finite element simulations with COMSOL® were performed based on the configuration shown Fig. 2. Two different values for the sphere radius R were considered (1 m and 10 cm) to represent both a large and a small object with varying heights above the ground (from 10 cm to 4 m). The field meter was modelled as a cylinder

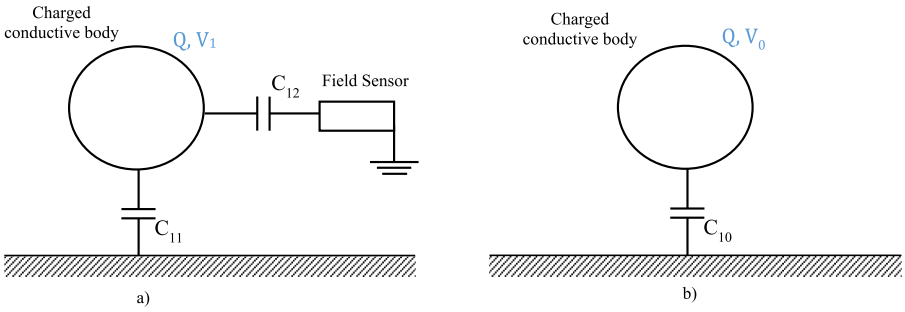

Fig. 1. A charged body in the presence of a grounded instrument (a) or standing alone (b) with the same electrostatic charge in both situations.

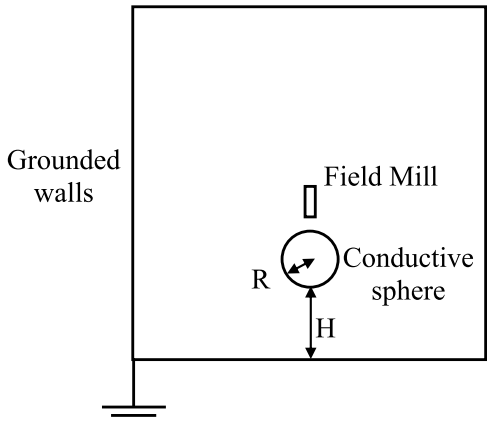

Fig. 2. Simulated configuration with Finite Elements.

with an 8 cm diameter and 14 cm height, positioned 10 cm above the sphere. The total simulated volume was a cylinder with a 10 m diameter and 10 m height. The sphere carried a constant charge of 100 nC.

The results are shown in Fig. 3. As expected, the presence of the grounded field meter reduces the potential of the sphere. The influence of the instrument is more significant for a small object (10 cm diameter), leading to a reduction in the electrostatic potential of up to 787 V (nearly 9 %) from an initial potential of 8818 V when the distance to ground is 4m. It is important to note that this is not a measurement error of the instrument, it is an influence the instrument exerts on the electrostatic configuration. For a larger sphere (1 m diameter), the influence of the field meter is much smaller (28.3 V or 4 % for an initial potential of 705 V at a distance of 4 m to the ground), even though the distance between the sphere and the instrument remained unchanged.

To further illustrate equations (4) and (5), capacitances have been calculated for the case were both spheres of 1m and 10 cm radius are at 4 m above ground. For the 1 m radius sphere, C_{10} = 136.35 pF and C_{11}+C_{12} = 141.82 pF which corresponds to a 4 % reduction in voltage. For the 10 cm radius sphere, C_{10} = 11.34 pF and C_{11}+C_{12} = 12.45 pF consistent with a 9 % reduction in voltage.

3.2. Influence of the feedback probe

The complexity of using a feedback probe increases from an electrostatic point of view because the sensor is not grounded. We can express the relationship using the capacitances shown in Fig. 4 (see Ref. [8]):

$$\begin{aligned} Q_1 &= C_{11}V_1 + C_{12}(V_1 - V_2) \\ Q_2 &= C_{22}V_2 + C_{12}(V_2 - V_1) \end{aligned} \tag{6}$$

Where Q_1 and Q_2 are the total charges of the sphere and the probe, V_1 and V_2 their absolute potentials, C_{11} the capacitance of the object to ground, C_{12} the capacitance between the object and the feedback probe and C_{22} the capacitance of the feedback probe to ground. For simplicity, we use the same symbol C_{11} to represent the capacitance between the object and the ground, whether in the presence of a feedback probe or a field mill, to avoid complicating the terminology. However, the values of C_{11} may differ in each case.

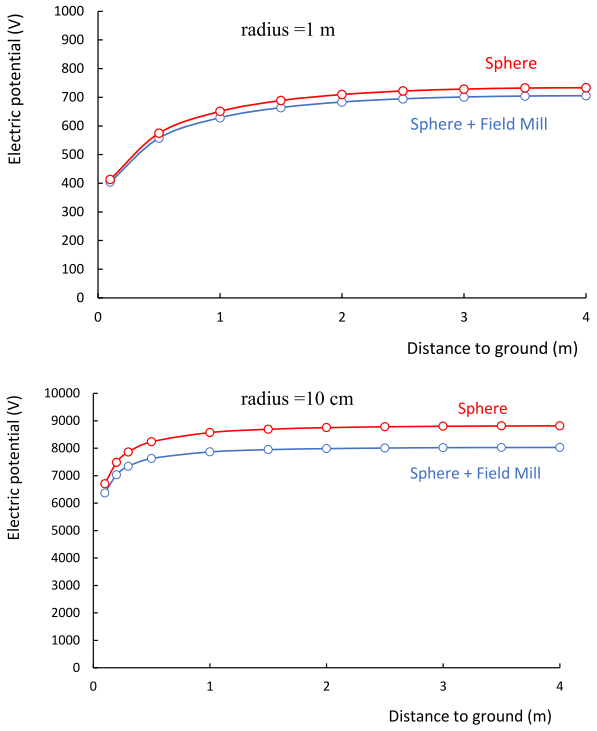

Fig. 3. Electric potential of different 100 nC charged spheres at a given distance of a ground plane, with or without a grounded field meter close (10 cm) to their surface.

Equation (6) can be rewritten as the Maxwell's matrix:

$$\begin{bmatrix} Q_1 \\ Q_2 \end{bmatrix} = \begin{bmatrix} C_{11} + C_{12} & -C_{12} \\ -C_{12} & C_{22}+C_{12} \end{bmatrix} \begin{bmatrix} V_1 \\ V_2 \end{bmatrix} \tag{7}$$

When the sphere is alone, we have:

$$Q_1 = C_{10}V_1 \tag{8}$$

The feedback probe removes some of the field lines connecting the sphere to the ground. Hence C_{11} is smaller than C_{10}. Additionally, since the probe ensures that $V_1 = V_2$, we have:

$$Q_1 = C_{11}V_1 \tag{9}$$

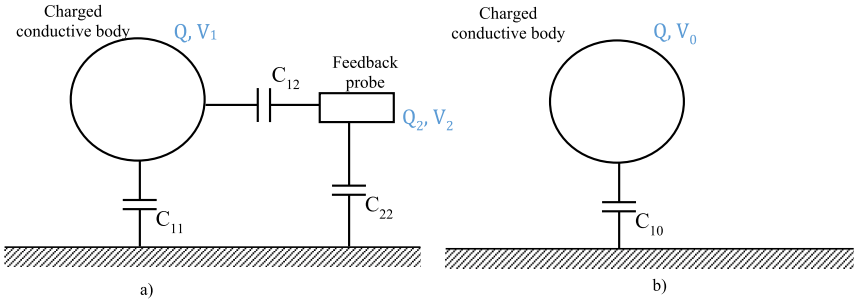

Fig. 4. A charged body in the presence of a feedback probe or standing alone.

A simulation was conducted, replacing the field meter in Fig. 2 by a cylindrical feedback probe of radius 1 cm and length 10 cm, positioned at distance 0.5 cm above the top of the sphere. As before, the spheres were assumed to carry a charge of 100 nC. The results of this simulation are shown in Fig. 5. When the feedback probe is present, the potential of the charged sphere increases, with a maximum rise of 381 V (+4.2 %) for an initial potential of 8818 V on the small (10 cm) sphere. However, if the object is strongly coupled to the ground, as in the case of the 1 m diameter sphere, the effect becomes negligible (0.08 %).

For a given charge on the floating object, the feedback probe tends to increase the electrostatic potential of the object being measured, whereas the field mill tends to reduce it. As a general conclusion for both measurement methods, the geometry of the problem must be carefully considered to ensure that the measuring instrument does not significantly alter the potential to be measured.

In the case of feedback probe, only objects with high capacitance to ground should be measured or, at least, the modification of the potential by the probe has to be evaluated. Although the electrostatic potential may be altered by the probe, the measured potential will still represent the actual potential of the object when the feedback probe is close. Thus, no calibration of the measurement is required.

Regarding the field mill, one strategy to avoid perturbing the potential of the floating object is to integrate the field mill into a flat conductive surface that is already part of the setup. In this configuration, the electrostatic potential of the floating conductive object will not be modified. However, this approach does not resolve the calibration issues discussed below. A field mill measures the electric field. Conversion of the measured electric field into the potential of the floating conductive object, requires a calibration.

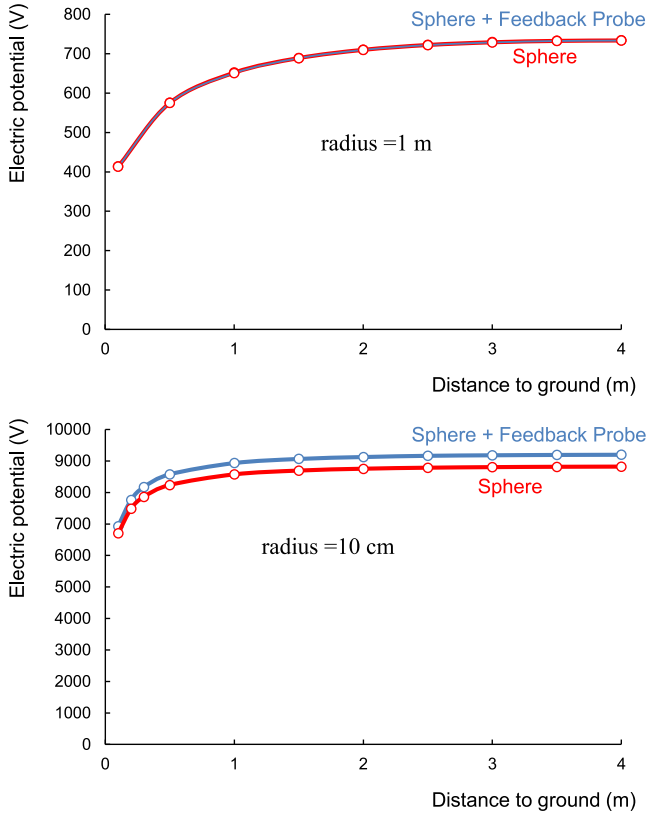

Fig. 5. Electric potential of 2 different radius 100 nC charged spheres alone and with a feedback probe close to their surface as a function of the distance to ground of the spheres.

4. Calibration of a field mill to determine the potential of charged floating objects

4.1. Electrostatic analysis of the problem

In many practical applications, only field mills can be used to measure the electrostatic potential of a floating object. The potential to be measured may be out of reach of a feedback probe, or the capacitance of the charged object may be too small to allow correct operation. To avoid any perturbation of the potential by the field mill, it can be integrated in an already existing ground plane, thus eliminating the problems described in section 3. Alternatively, the field mill can be integrated into the conductive surface of the floating object, as is commonly done with aircrafts.

If the geometry of the problem is well known, the electrostatic potential can be obtained from the measurement of the electric field by calculation or by finite elements simulation. However, it is often more convenient to calibrate the experimental setup by charging the floating object to a known potential using an external high voltage generator.

However, this introduces a third element, namely the high-voltage generator cable. Two scenarios may arise: either the cable is a bare conductor (Fig. 6a), or it is shielded with a grounded screen (Fig. 6b). We used the following convention: one or two apostrophes follow the capacitance names to differentiate them from those in Fig. 1a. One apostrophe refers to calibration with an unshielded cable and two apostrophes refer to calibration with a shielded cable.

For calibration with an unshielded cable.

- C'_{11} is the capacitance of the object to ground.
- C'_{12} is the capacitance between the object and the field mill.
- C'_{23} is the capacitance between the unshielded cable and the field mill.
- Q'_1 is the total charge of the conductive floating object.

And for calibration with a shielded cable.

- C''_{11} is the capacitance of the object to ground.

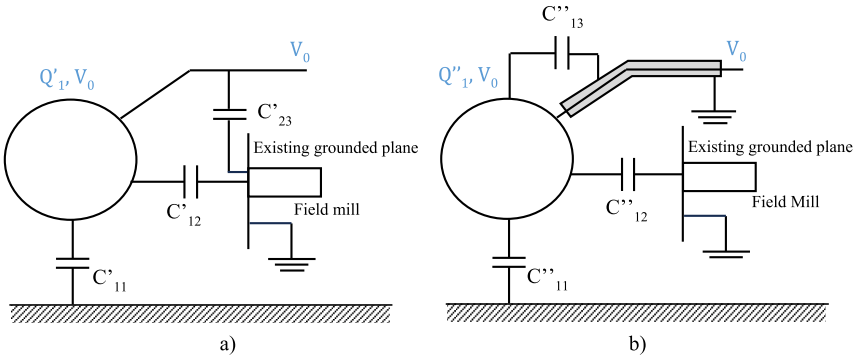

Fig. 6. Measurement of an electrostatic potential by a field mill integrated in an existing grounded plane: calibration of the setup by using an unshielded cable (a) or a shielded cable (b).

- C''_{12} is the capacitance between the object and the field mill.
- C'_{13} is the capacitance between the object and the grounded screen of the cable.
- Q''_1 is the total charge of the conductive floating object.

In both cases, the cable core and the object are polarized at the calibration potential V_0.

Note that we are considering the case where the field mill is integrated into an existing grounded plane to avoid modifying the potential of the object, but the following analysis also applies to cases where the field mill is not integrated into such a conductive surface. The only difference would be the modification of the floating object's potential compared to the situation of the sphere alone.

In the case of the unshielded cable (Fig. 6a), the cable introduces two effects.

- The cable reduces the capacitance between the sphere and the ground ($C'_{11} < C_{11}$) if it crosses field lines connecting the sphere to ground. As a result, for a potential V_0, the charge on the sphere will be smaller $(Q'_1 < Q)$. When the cable is removed, the sphere's potential will be less than V_0.
- The cable affects the field mill measurement in two ways: (1) it introduces a capacitance C'_{23} which increases the electric field measured by the field mill by a factor of $(C'_{12} + C'_{23})/C_{12}$ and (2) it reduces the C'_{12} capacitance compared to the C_{12} capacitance. Both effects can be minimized by placing the field mill as far away as possible from the influence of the cable.

In the case of the shielded cable (Fig. 6b), three main differences arise.

- The direct influence of the cable on the field mill represented by C'_{23} disappears.
- By bringing the grounded shield of the cable close to the sphere, a capacitance C''_{13} is introduced increasing the total sphere to ground capacitance $(C''_{11} + C''_{13} > C_{11})$. As a result, the charge of the sphere at potential V_0 is also increased $(Q''_1 > Q)$. When the cable is removed, the sphere's potential will be higher than V_0. This can cause a significant increase in potential.
- The capacitance C''_{12} is reduced compared to C_{12} because the shield attracts some of the field lines, reducing the charge induced on the field mill and the measured electric field.

4.2. Finite elements modelling

Let us consider a conductive sphere floating above the ground, charged by a cable connected to a high voltage source of 5 kV, as represented in Fig. 7. Three possible positions of the cable are represented. We assume that the field mill is integrated in the ground or in the sphere in a way that it does not disturb the electric field (a typical configuration for aircraft measurements), thus avoiding the perturbations analyzed in section 3.1. The connecting cable may or may not be shielded with a grounded mesh, as shown in Fig. 6.

The finite elements model is represented in Fig. 8 for the case of the vertical cable. Both spheres are represented simultaneously to show their relative position and the constant distance to ground, but both cases are calculated separately, with the cable in contact with the sphere in each scenario. The conductor diameter is 1 mm, and the cable's insulation layer has a diameter of 10 mm. The outer surface of the insulating layer is grounded in the case of the shielded cable. The distance from the shield to the sphere or the tip of the cable is 4 cm. Calculations are performed with COMSOL ®.

Results are shown in Tables 1 and 2 for an unshielded and shielded cable respectively, for spheres of radius 1 m and 10 cm. The measured electric field strongly depends on the cable's position. With the unshielded cable (Table 1), the electric field measured by the sensors for the 10 cm radius small sphere can be up to roughly 3 times higher (+180,4 %) than the electric field of the sphere alone. For the 1 m radius sphere, the maximum difference is about +7.5 %. When a shielded cable is used (Table 2), the problem is mitigated for the small sphere, where the maximum difference is −23.15 %. For the large sphere, the maximum difference is around −7.6 %.

In any configuration, while the cable is touching the sphere, the potential of the sphere is 5 kV. However, the measured electric field does not correspond to the electric field of a floating conductive sphere alone

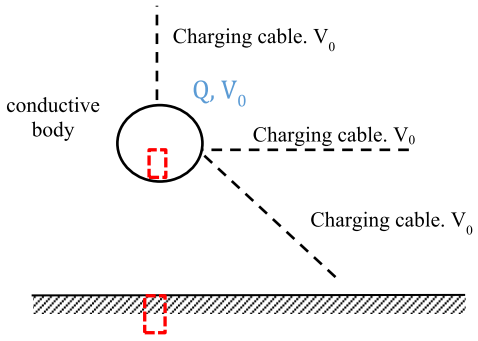

Fig. 7. A floating sphere charged by a cable connected to a voltage source V_0 in 3 different positions. In red, 2 positions of a field mill: in the ground or inside the sphere. (For interpretation of the references to colour in this figure legend, the reader is referred to the Web version of this article.)

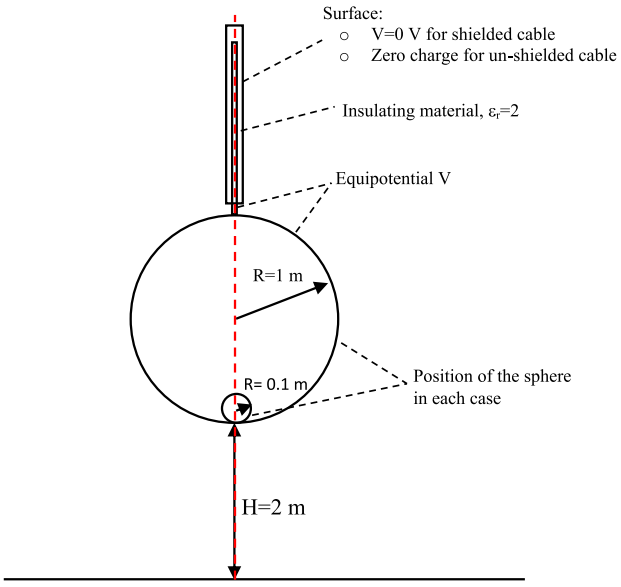

Fig. 8. Dimensions of the Finite Elements model for the vertical cable case.

Table 1
Electric field (V/m) calculated in the internal sensor or the ground sensor for an unshielded contacting cable and a sphere and/or cable potential of 5 kV.

	Radius = 1m		Radius = 10 cm	
	Ground sensor	Internal sensor	Ground sensor	Internal sensor
	1351.6	6712.55	228.94	50343
	1370	6494.8	425.1	45187
	1352.7	6590.1	349.42	47155
	1453.3	6360.9	642	41056

Table 2
Electric field (V/m) calculated in the internal sensor or the ground sensor for a shielded contacting cable and a sphere and/or cable potential of 5 kV.

	Radius = 1m		Radius = 10 cm	
	Ground sensor	Internal sensor	Ground sensor	Internal sensor
	1351.6	6712.55	228.94	50343
	1330.3	6606.4	193.02	53563
	1340.4	6624.4	203.56	52399
	1284.8	6888	175.95	57868

at a potential of 5 kV, and the electrostatic charge of the sphere also differs from the case of the sphere alone. These calculations clearly show that converting the field measured by the instrument into a potential will lead to erroneous values, regardless of the calibration method used, unless a correction is applied.

Let us consider the situation described Fig. 9 where a 10 cm radius sphere is 2 m above the ground, charged at 5 kV. In case (A), where the sphere is alone, the electric field induced in the ground sensor below the sphere is 228.94 V/m (Table 2) and the total charge on the sphere is 57 nC. During calibration at the same potential with an unshielded horizontal cable (B), which is a common calibration method, the measured electric field in the sensor is 1.84 times higher (425.1 V/m), while the sphere charge is only 48.6 nC. After the cable is removed (C), the sphere's potential drops to 4.26 kV, with a measured field in the sensor of 195.2 V/m. If situation (B) is taken as the reference for calibration, 425.1 V/m would be incorrectly taken as the electric field corresponding to a potential of 5 kV. After the cable is removed, the potential of the sphere alone, calculated from the electric field measured by the field mill (195.2 V/m) and taking as a reference the electric field at B (425.1 V/m), would be $195.2/425.1 \times 5 = 2.29$ kV. This represents an error of −46 % from the real potential of the sphere (4.26 kV). Conversely, if one considers that the true value of 5 kV is obtained in (C) when the cable has been removed, the error would be about +17 % of the real potential of the sphere. Neither scenario is suitable for calibration.

If a shielded cable is used (Fig. 10), the situation does not improve, as the sphere's charge in (B) at 5 kV will be very high (611.73 nC) due to the proximity of the grounded shield. The electric field at the sensor is then 193.02 V/m. After the cable is removed (C), the sphere's potential rises to 53.6 kV with an electric field of 2457 V/m at the sensor's position. Calibration in (B) would lead to the incorrect conclusion that the potential in C is 63.6 kV (+18.6 %), while calibration in (C) (2457 V/m for 5 kV) would result in an error of −90.7 %.

These significant errors represent a "worst case" scenario to illustrate the calibration problem, but they can be greatly reduced by several factors. First, the sphere's diameter and distance to the ground play a decisive role in calibration errors, which are much lower for larger spheres. Second, the cable's position is critical. Even a bare cable placed on the opposite side of the sphere from the sensor has a significant impact when considering a small sphere, as it reduces the field

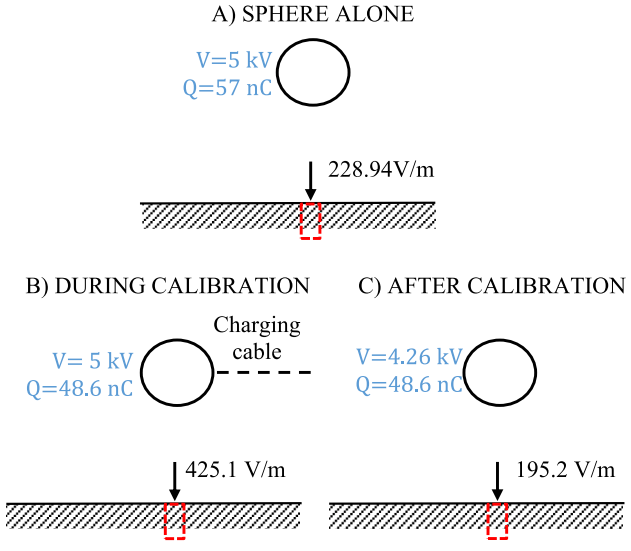

Fig. 9. Comparison of the theoretical situation of a 10 cm radius sphere charged at 5000V and the process of calibration with an unshielded horizontal cable touching the sphere (in red, the position of the field mill). (For interpretation of the references to colour in this figure legend, the reader is referred to the Web version of this article.)

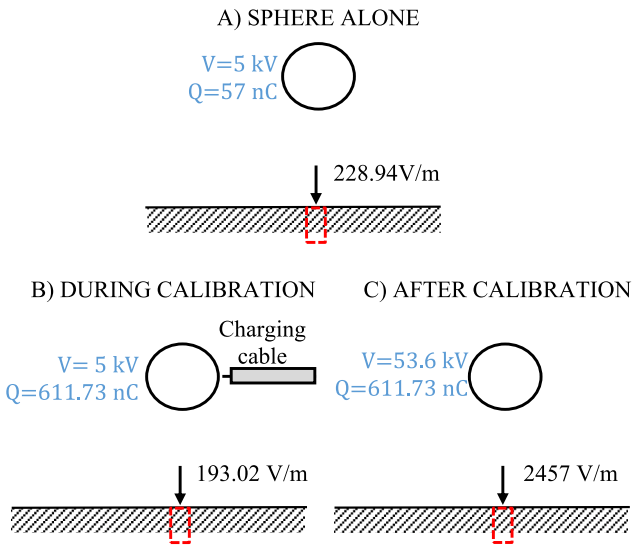

Fig. 10. Comparison of the theoretical situation of a 10 cm radius sphere charged at 5000V and the process of calibration with a shielded horizontal cable touching the sphere (in red, the position of the field mill). (For interpretation of the references to colour in this figure legend, the reader is referred to the Web version of this article.)

concentration produced by the sphere, decreasing the field on its surface while increasing the field induced in the ground sensor (Fig. 11).

Therefore, 3D modelling of the problem should be carried out in many practical cases to obtain the correct calibration constant.

5. Experimental measurements and modelling

5.1. Experimental setup

These situations have been experimentally tested in the laboratory using an experimental setup with a magnetic levitation system, as described in Fig. 12 (a similar setup can be found in Ref. [9]). The object levitates between two horizontal grounded discs, each with a diameter of 20 cm, separated by 8.5 cm. A field mill is integrated into the upper disc. The magnet has a conductive surface on top or is placed inside a metallic box. The conductive surface of the magnet or the metallic box are electrically charged to 1.5 kV by touching it with a high-voltage generator cable. The entire setup is housed in a closed metallic box to prevent any external disturbances.

In our experiments, the field mill had to be positioned at least 5 cm away from the magnet to avoid significant noise in the measurements caused by the magnetic fields of the levitation system. The charging cable is introduced horizontally, and the last 10 cm of the cable are unshielded. For measurements simulating the use of a shielded cable, a metallic shield was added near the end of the cable.

5.2. Measurements during calibration

The electric field measured by the field mill when the magnet is charged with an unshielded cable is shown in Fig. 13. With the unshielded cable, the measured electric field is higher during contact with the cable than in the theoretical case of the magnet alone charged at 1.5 kV without any cable. After the contact, the measured field is

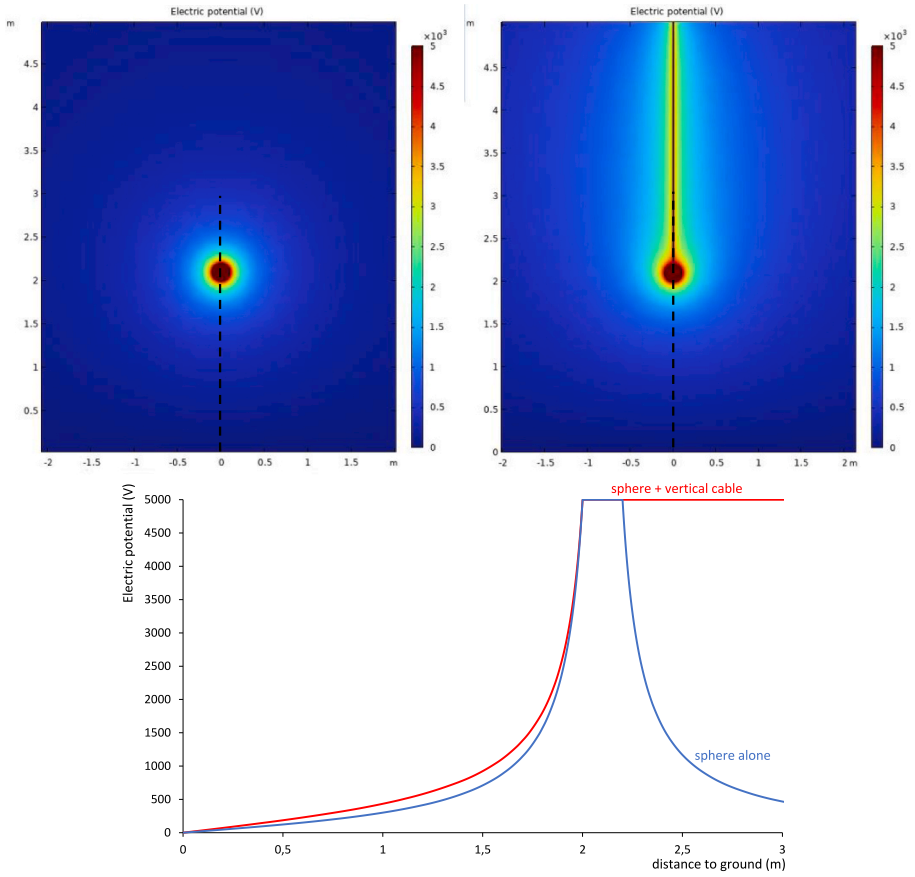

Fig. 11. Electric potential distribution for the case of a small sphere (10 cm radius) alone and for the same sphere with a vertical unshielded cable in contact. The figure below shows the potential distribution along the dashed lines for both cases.

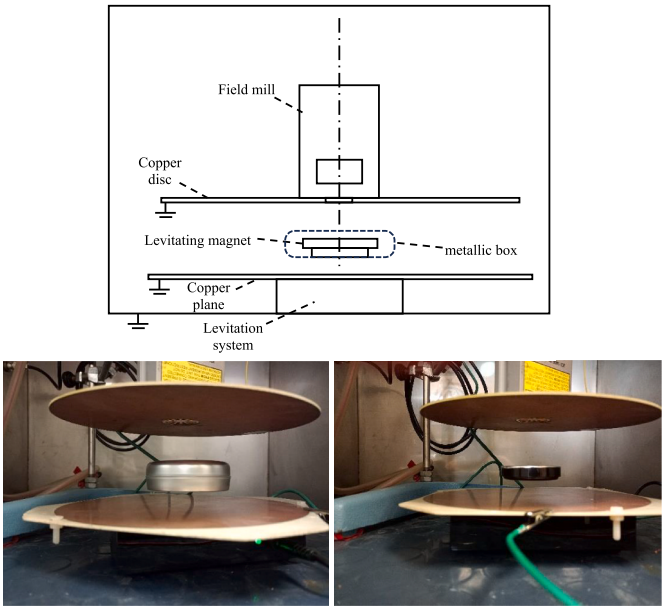

Fig. 12. Drawing and picture of the experimental setup of a floating conductive object.

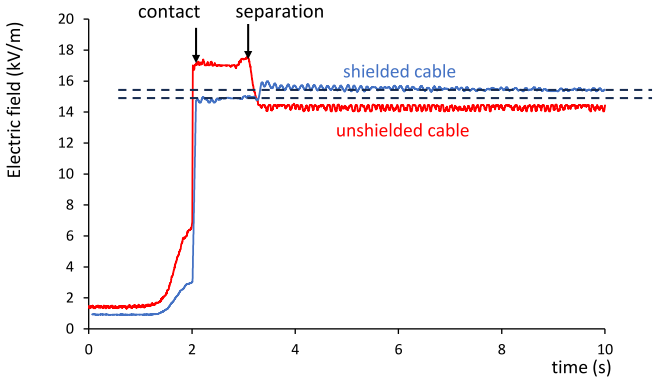

Fig. 13. Evolution of the electric field measured during contact and separation of the shielded and unshielded cable a 1.5 kV with the magnet.

lower than the theoretical case, as the transferred charge is reduced. In contrast, with the shielded cable, the opposite occurs. The two black dashed lines indicate the approximate range where the electric field generated by the magnet alone, charged to 1.5 kV, is expected to lie. In this case, the best approximation is obtained using the shielded cable.

In the case where the magnet is placed inside the metallic box, the capacitance to ground of the floating object is higher, and the disturbances caused by the cable are smaller, as shown in Fig. 14. These measurements are closer to the case of the floating object charged at 1.5 kV alone (the dashed lines roughly indicate the possible range of the electric field in this case).

5.3. Finite elements modelling

The case of the magnet inside the metallic box has been simulated using finite elements (Fig. 15). This configuration was chosen instead of the magnet without the metallic box because the magnet's surface is insulating, and the distribution of charges on its surface (which is unknown and variable) influences the experimental results, making comparison with the simulation more challenging.

The simulations provide the electric field at the position of the field mill and the charge on the floating object when it is in contact with the

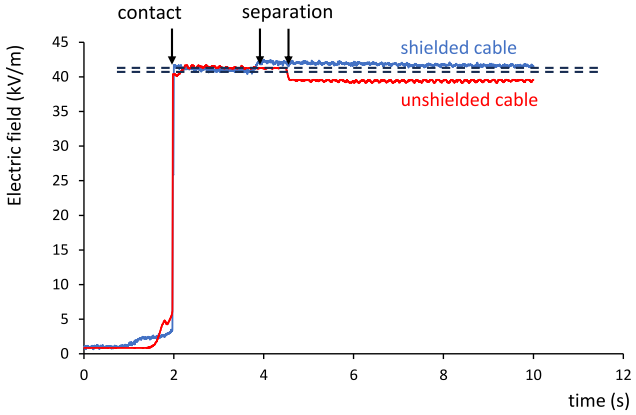

Fig. 14. Evolution of the electric field measured during contact and separation of the shielded and unshielded cable a 1.5 kV with the magnet inside the box.

cable. From this, the electric field created by the floating object with the charge transferred during contact can be calculated once the cable is removed. This is represented in Fig. 16 and detailed in Table 3. Although the simulations are electrostatic, we have represented the results as a function of time to visually compare them with the experimental measurements.

The values are in fairly good agreement with the experimental measurements (Fig. 14). The differences arise from simplifications in the geometry and the difficulty of precisely measuring the distances in the experimental setup. In this case, the dashed line represents the electric field created by the floating object charged to 1.5 kV, confirming that it always lies between the shielded and unshielded cable measurements.

Following the naming of sections 3 and 4, in our simulation the capacitance to ground of the metallic box alone was $C_{11} + C_{12} = 7.83$ pF. The capacitance of the metallic box to ground with the unshielded cable was $C'_{11} + C'_{12} = 7.66$ pF and the capacitance of the metallic box to ground with the shielded cable was $C''_{11} + C''_{12} + C''_{13} = 8.11$ pF. This is consistent with the observed results.

Next, the error introduced by using situation B or C of Fig. 9 or Fig. 10 as the calibration point is calculated in Table 3. In the first row of the table, the case of the magnet inside the metallic box charged to 1500 V was used as a reference. The charge on the metallic box and the electric field at the field mill were calculated. Then, both charging scenarios—using shielded and unshielded cables—were simulated, and the charge on the metallic box was calculated for each one. It was assumed that the charge on the metallic box remained the same after the cable was disconnected. With this charge, the new electric field at the field mill and the new potential of the box after cable disconnection were calculated. This allowed us to estimate the error in determining the potential of the metallic box if it was assumed that the metallic box potential was 1500 V during cable contact or after cable contact. In this case, the errors are small because the capacitance of the object to ground is relatively high. The maximum error is here −3.45 %. In both cases, calibration during contact is the better option.

5.4. Potential decay

A long-term measurement of the potential decay of the magnet with the metallized top face was performed. It was charged using a horizontal unshielded cable.

The reference for the measurement calibration is taken as the potential after the separation of the cable and the magnet (Fig. 17), as it provides the best approximation, according to Fig. 13.

The potential decays of the magnet for charging potentials of 1 kV, 2 kV, 3 kV and 4 kV are shown in Fig. 18. The curve corresponding to 4 kV is dashed because it is a trend line obtained from raw data. For this charging voltage, a scale adjustment had to be made on the field mill,

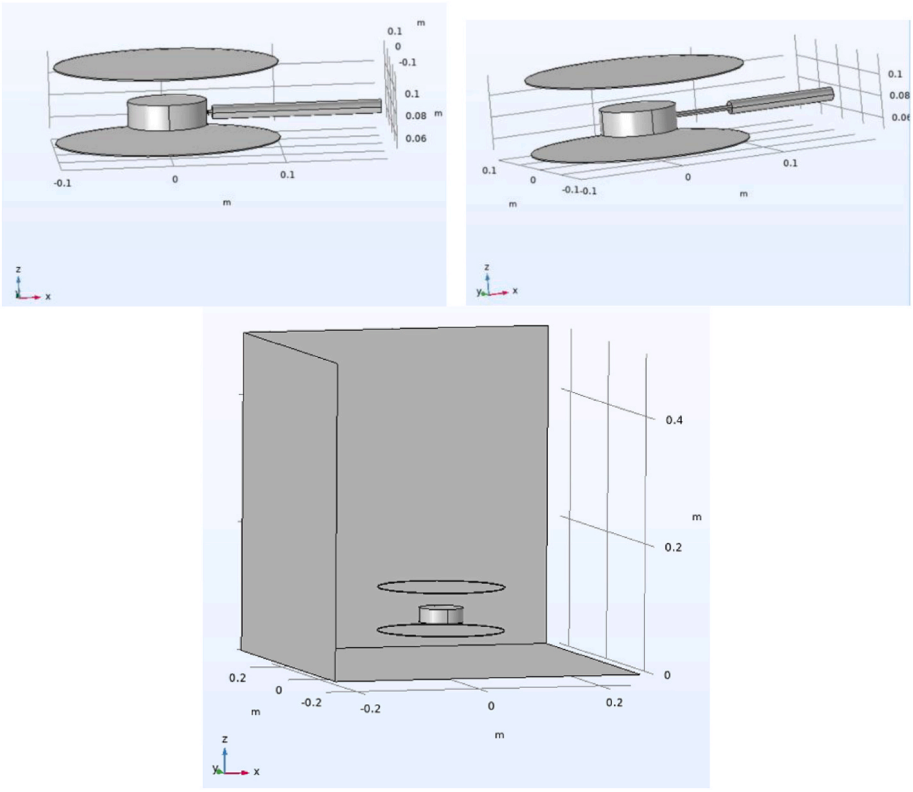

Fig. 15. Model of the magnet inside a metallic box with the shielded, unshielded cable and alone (the external enclosure is only partially represented in the third case for the sake of clarity, but it was present in all the cases).

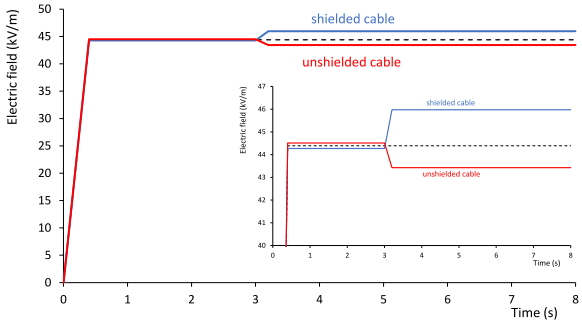

Fig. 16. Calculated values of the electric field for the case of the magnet inside the metallic box. The dashed line corresponds to the floating object alone charged at 1.5 kV.

resulting in poor vertical resolution.

For voltages below 3 kV, the shape of the decay curve is a straight line. A similar result, with slopes independent of the material, has been reported for potential decay controlled by gaseous neutralization on thick epoxy and Teflon insulators in SF6 [10]. In experiments using an electromagnetic levitation system [9], a linear decay was also observed, with a typical slope of about 100 V per day, depending on the environment but independent of the surface voltage. However, at low fields, a decay following a power-law in time was observed, which is absent in our experiments.

The linear shape of the decay suggests that the levitating magnet is discharging with a constant current:

$$i_{discharge} = C\frac{\Delta V}{\Delta t} \tag{10}$$

where C is the total magnet capacitance to the grounded planes, which is approximatively:

$$C \approx \left(\frac{1}{d_1}+\frac{1}{d_2}\right)S\varepsilon_0 \tag{11}$$

Where S is the horizontal surface of the magnet while d_1 and d_2 are the distances of the magnet to the upper and lower grounded planes, respectively.

The constant discharge current over time, and its weak dependence on the magnet's voltage, suggests that the current is controlled by a process independent of the potentials and fields generated by the charged magnet. This process is most likely ion generation in the vicinity of the magnet, with the weak field dependence indicating that a complete collection of ions is achieved within a defined volume during the time scale of the experiment.

Ions may be produced by ionizing radiation, such as cosmic rays and terrestrial radioactivity, or by electrical discharges. Without electrical discharges, a typical generation rate g is 10 ions $s^{-1}cm^{-3}$ [11]. Assuming g remains constant over time, the current flowing to a charged area is proportional to the collection volume $\mathscr{V}$, in which the ions are drained by this charged area:

$$i_{discharge} = ge\mathscr{V} \tag{12}$$

Where g is the ion generation rate and e is the charge of an electron. Therefore:

$$g = \left(\frac{1}{d_1}+\frac{1}{d_2}\right)\frac{S\varepsilon_0}{e\mathscr{V}}\frac{\Delta V}{\Delta t} \tag{13}$$

From Fig. 18, for a charging potential of 1 kV, $\Delta V/\Delta t = 1000/$

Table 3
Summary of the results obtained by simulation.

	Electric field at field mill (V/m)	Charge on the metallic box at 1.5 kV (nC)	Electric field after removing the cable (V/m)	Potential of the metallic box after removing the cable (V)	Deduced potential after separation if calibrated …	
					… during contact (B case) (V)	… after separation (C case) (V)
Magnet in the metallic box alone	44387	11.741	44387(*)	1500(*)	–	–
Charging with shielded cable	44268.5	12.161	45974.82	1553.66	1557.82 (+0,27 %)	1500 (−3.45 %)
Charging with unshielded cable	44510	11.487	43426.75	1467.55	1463.49 (−0.28 %)	1500 (+2.21 %)

(*) This is the reference case of the metallic box charged at 1500 V, no cable is present.

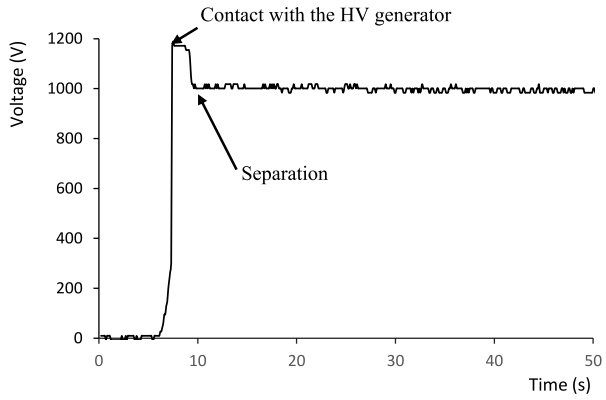

Fig. 17. Scaled measurement of the first 40 s after charging the floating conductive object at 1 kV. Calibration point is taken after separation.

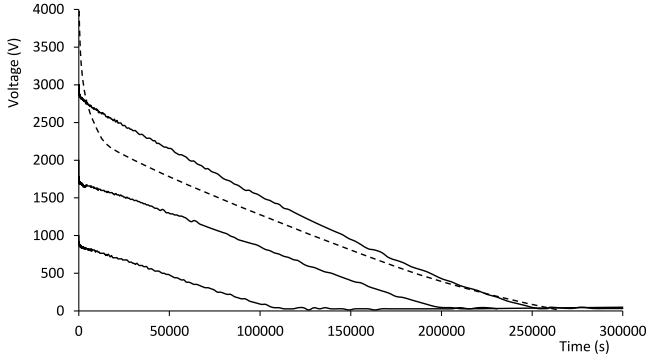

Fig. 18. Potential decay curves for 1 kV, 2 kV, 3 kV and 4 kV (the 4 kV is represented with a dashed line because it is a trend curve due to the poor resolution of the field mill at this scale).

113000 V/s. Here $d_1 = 1.3\ cm, d_2 = 3\ cm, S = 28.3\ cm^2$. Assuming g to be 10 ions $s^{-1}cm^{-3}$, the collection volume of the charged magnet would be:

$$\mathscr{V} = \left(\frac{1}{d_1}+\frac{1}{d_2}\right)\frac{S\varepsilon_0}{eg}\frac{\Delta V}{\Delta t} = 15200\ cm^3 \quad (14)$$

The volume between the electrodes is 2670 cm^3, while the total volume of the Faraday cage surrounding the setup is 125000 cm^3. The order of magnitude obtained for the collection volume appears to be correct, although it is difficult to be more precise. In Ref. [11], the saturation occurs when the field exceeds 30 V/m. Using this criterion, we attempted to compute the collection volume with a field simulation. However, the obtained result suggests that the collection volume, and thus the current, should strongly depend on the magnet's potential. This is not consistent with our observations, which may be because the 30 V/m criterion does not apply in this case, or it could be due to insulating parts present near the electrodes in our experiments, which may have become charged and limited the expansion of the collection volume. This would also explain why our decay curves tend to be more linear than what has been reported in Ref. [9]. More experimental and theoretical work is needed to clarify this. A first step could be confining the experiment in a small metal box to ensure the collection volume remains constant throughout most of the decay, allowing for a more accurate estimation of g, which may then be used to evaluate the collection volume in other environments.

For the 4 kV charging voltage in Fig. 18, there is a rapid decay during the first 1000 s, likely due to corona discharges from the magnet. After this, the potential decay resumes a linear trend below the 3 kV line. This "crossover" phenomenon may be attributed to electron emission or corona pulses near the magnet during charging and the initial discharging phase.

6. Conclusion

The influence of electrostatic instruments such as field mills, short-term measurement field meters, or feedback probes must be carefully considered when analyzing the electrostatic potential of an object. Special attention is required when dealing with floating conductive objects. In general, feedback probes have a smaller impact on the potential of the object. Integrating a field mill into the ground or a flat grounded surface produces no influence on the electric field or potential of the floating object. If the potential measurement is conducted with a field mill, the calibration constant between the electric field and electrostatic potential must be determined. Experimental calibration, performed by applying a known potential to the floating object, must be carried out with care. The influence of the charging cable must also be assessed. As a general rule, a 3D finite element simulation is a valuable tool for achieving accurate calibration of the system [12], provided that all geometrical parameters and material properties of the experimental setup are well known. Caution should be exercised when calibrating the measurement and converting the value delivered by the field mill in V/m into the electrostatic potential of the analyzed object. The use of shielded cables for charging objects is recommended, especially for objects with a large capacitance to ground. Charging with both shielded and unshielded cables can also help in obtaining a more accurate estimate of the calibrated voltage.

CRediT authorship contribution statement

Pedro Llovera-Segovia: Writing – review & editing, Writing – original draft, Visualization, Software, Resources, Methodology, Investigation, Formal analysis, Data curation, Conceptualization. **Philippe Molinié:** Writing – review & editing, Writing – original draft,

Methodology, Investigation, Formal analysis, Conceptualization. **Vicente Fuster-Roig:** Writing – review & editing, Supervision, Software, Resources, Investigation, Data curation. **Alfredo Quijano-López:** Writing – review & editing, Supervision, Resources, Methodology, Investigation.

Declaration of competing interest

The authors declare that they have no known competing financial interests or personal relationships that could have appeared to influence the work reported in this paper.

Data availability

Data will be made available on request.

References

[1] B.C. Martell, P. Fontanes, J. Montanyà, C. Guerra-Garcia, Flight demonstration of net electric charge control of aircraft using corona discharge, IEEE Trans. Aero. Electron. Syst. 58 (Nº 6) (2022) 5607–5618.
[2] P. Molinié, P. Llovera, Surface potential measurements: implementation and interpretation, in: 2000 Eighth International Conference on Dielectric Materials, Measurements and Applications vol. 473, IEE Conf. Publ. No., 2000, pp. 253–258.
[3] P. Molinié, "How Fast Does a Static Charge Decay? an Updated Review on a Classical Problem", this issue.
[4] J.S. Chang, A.J. Kelly, J.M. Crowley, Handbook of Electrostatic Processes, Marcel Dekker Inc., New York, 1995.
[5] J.N. Chubb, Calibration of Instruments for Electrostatic Measurements, IEE Colloquium on Significance of Calibration, 1993.
[6] P. Llovera, P. Molinié, A. Soria, A. Quijano, Measurements of electrostatic potentials and electric fields in some industrial applications: basic principles, Journal of Electrostatics Nº 67 (2009), 457–46.
[7] R. Kacprzyk, Measurements of electrical potential of constant charge objects, IEEE Trans. Dielectr. Electr. Insul. 19 (1) (2012) 134–139.
[8] M.N. Horenstein, Measuring isolated surface charge with a noncontacting voltmeter, Journal of Electrostatics Nº 35 (1995) 203–213.
[9] C. R Heinert, R. Mohan Sankaran, D.J. Lacks, Decay of electrostatic charge on surfaces due solely to gas phase interactions, Journal of Electrostatics N°115 (2022) 103663.
[10] T.J.M. Gaertner, Th Stoop, J. Tom, H.F.A. Verhaart, A.J.L. Verhage, Decay of surface charges on insulators in SF6, in: 1984 IEEE International Conference on Electrical Insulation, IEEE, Montreal Quebec, Canada, 1984, pp. 208–213, https://doi.org/10.1109/EIC.1984.7465181.
[11] J. Kindersberger, C. Lederle, Surface charge decay on insulators in air and sulfurhexafluorid-Part I: simulation, Dielectrics and Electrical Insulation, IEEE Transactions On 15 (2008) 941–948.
[12] T. Takuma, M. Yashima, T. Kawamoto, Principle of surface charge measurement for thick insulating specimens, IEEE Trans. Dielectr. Electr. Insul. 5 (N°4) (1998) 497–504.